Hindawi
Journal of Control Science and Engineering
Volume 2018, Article ID 3582454, 8 pages
https://doi.org/10.1155/2018/3582454

Research Article

The Characteristic Improvement of Electromagnetic Proportional Directional Control Valve

Hua Zhang

School of Mechanical Engineering, Anhui Science and Technology University, Fengyang, China

Correspondence should be addressed to Hua Zhang; chinafeihong@163.com

Received 16 May 2018; Accepted 27 August 2018; Published 6 September 2018

Academic Editor: Manuel Pineda-Sanchez

The electromagnetic proportional directional control valve is widely used in hydraulic control system and its typical faults are not enough electromagnetic force and too high temperature rise to burn out the coil. The magnetic field and coil temperature field distribution of the control valve are modeled and analyzed by using the finite element method. The influence laws of the geometry and parameters on electromagnetic force are analyzed. Furthermore, the influence of coil control current and heat transfer coefficient on the temperature rise of coil is analyzed, which provides a theoretical basis for the reliability optimization design of electromagnetic proportional directional control valve.

1. Introduction

Electromagnetic proportional directional control valve is widely used in electrohydraulic control systems. For example, by using the electromagnetic proportional directional control valve controlled hydraulic motor power system on flexible intelligent sprayer chassis developed by the author, chassis speed control and steering functions are realized. It is an essential component of electrohydraulic control system with high price and failure rate. The main failure forms are that the electromagnetic force is not enough [1] and the overheat of the coil, which leads to the malfunction of the control valve core. The traditional analysis method adopting simplified model, which leads to poor analysis accuracy, is not suitable for nonlinear and complicated parameter analysis of electromagnetic control valve [2]. Mechanical optimization design method emphasizes only on parameters optimization; the geometry optimization could not be accomplished [3–6]. The finite element method does not need complicated mathematical model but the accurate physical model and boundary conditions. Therefore, the finite element method for electromagnetic field and thermal analysis theory are adopted in order to solve the parameters and geometry optimization problem. The changing regulation and influence factors of electromagnetic force and the temperature rise of the coil are explored.

2. Electromagnetic Field Analysis of Electromagnetic Proportional Directional Control Valve

The electromagnetic proportional directional control valve adopted in flexible intelligent sprayer chassis is PRM2-06-3Z11. Brand is ARGO-HYTOS. The structure is shown in Figure 1.

The electromagnetic proportional directional control valve drives the control valve core mainly by the electromagnetic force between the electromagnet coil and the armature. The stroke of the control valve core is proportional to coil current in theory and the electromagnetic force changes with the stroke of the control valve core [7]. After the current is off, the reset spring is used for resetting. Taking the electromagnet part of the control valve as the analysis object, the electromagnet structure diagram is set up, as shown in Figure 2.

Electromagnetic field theory and finite element method are used to analyze the electromagnetic field.

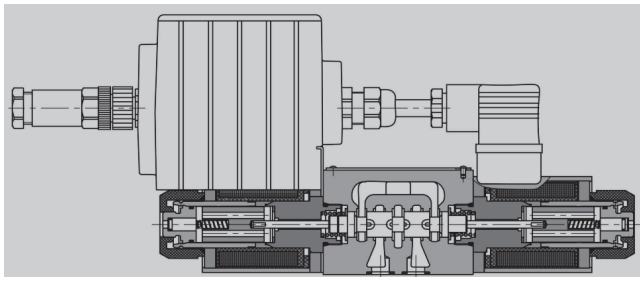

Figure 1: Structure of electromagnetic proportional directional control valve.

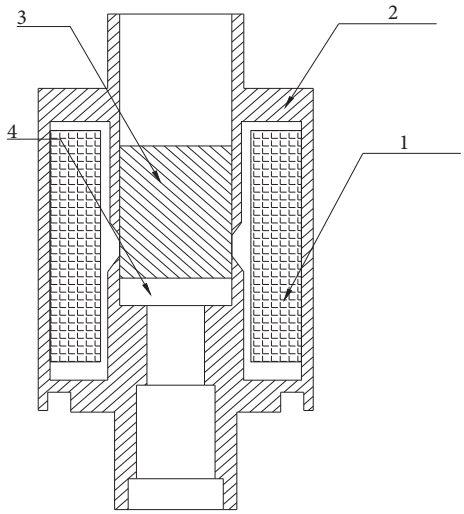

Figure 2: Electromagnet structure. (1) Coil; (2) iron core; (3) armature; (4) air gap.

(1) Preprocessing.

Since the proportional electromagnets are axisymmetric, the two-dimensional axisymmetric analysis method is used in ANSYS. Only half model is required and the whole model can be obtained by mirror [8] when modeling. The element type is set as PLANE13. The relative permeability of air and coil is set as 1 and that of iron core and armature is 2000. Half model is divided into quadrilateral mesh, as shown in Figure 3.

The armature is defined as an element and a magnetic force boundary condition is added. The current density load is applied to the coil as

$$J = \frac{NI}{A_{COIL}} \tag{1}$$

where N is coil turns. I is the current intensity of the coil. A_{COIL} is coil cross-sectional area.

In this paper, the coil turns of control valve are 10000, the current intensity is 1, the range of current value is 0.004-0.02A, and the cross-sectional area of the coil is 0.015m $*$ 0.05m.

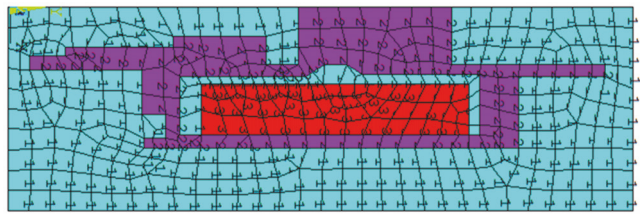

Figure 3: The proportional electromagnet meshing.

Parallel condition of magnetic flux lines is applied to all external nodes.

(2) Solution.

Static electromagnetic field analysis solver is used to solve the problem.

(3) Postprocessing.

View the results of the solution. The solution is shown in Figure 4.

The internal magnetic flux tends to be dense with the increase of current intensity. The magnetic flux is mainly distributed in the gap between the coil and the iron core and the armature when the current intensity reaches the maximum value. There are no closed magnetic flux lines through the iron core and the armature, as shown in Figure 4(a).

Electromagnetic force is calculated using the principle of virtual displacement:

$$F = \lim_{\Delta x \longrightarrow 0} \frac{\Delta W'}{\Delta x} = \frac{dW'}{dx} = -\left[\left(\frac{E_{x+\Delta x} + E_x}{\Delta x}\right)\right] \tag{2}$$

where $\Delta W'$ is the required energy. $\triangle x$ *is* displacement. E_x is system energy at zero displacement point. $E_{x+\Delta x}$ is system energy at the expected armature position.

As a result of ANSYS, the electromagnetic force is 40.75N when the coil current is 0.02A and the direction is -Y. The electromagnetic force is 0.19966N when the coil current is 0.004A and the direction is -Y.

(4) Optimization design.

Power consumption and electromagnetic force are the two important factors of electromagnetic control valve design. Power consumption is reduced usually by changing the coil turns and line diameter while ensuring that the electromagnetic force is enough [9]. But the number of turns and the coil diameter have a comprehensive influence on the force and power consumption. The increase of coil turns can increase the electromagnetic force [10], but it will lead to remarkable temperature rise of the coil. This is not conductive to improve the reliability of the control valve. In addition, the diameter of the coil will also affect the response characteristics of the control valve [11]. Therefore, methods are studied to increase electromagnetic force considering coil current and electromagnet geometric dimension.

① *Analysis of the influence of different current intensity on electromagnetic force.*

Under four different coil current intensities, 0.004A, 0.01A, 0.015A, and 0.02A, the electromagnetic force is

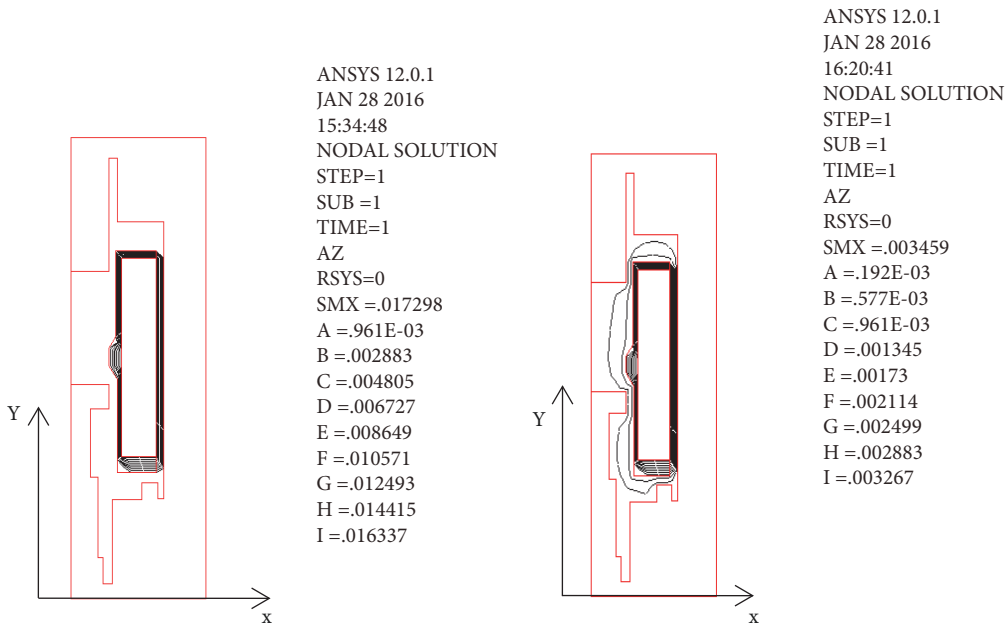

(a) $I = 0.02$A (b) $I = 0.004$A

Figure 4: Distribution of magnetic flux lines.

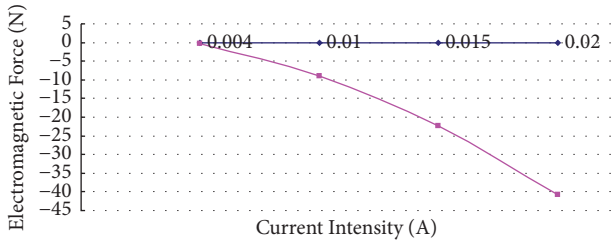

Figure 5: Curve of electromagnet force changes with current intensity.

calculated with the virtual displacement principle in ANSYS. The changing curve is generated as shown in Figure 5.

The electromagnetic force of the coil increases linear with the increase of the coil current intensity as shown in Figure 5.

② The influence of armature length on electromagnetic force.

30 mm, 40 mm, and 60 mm of armature length are selected to compare and analyze in the vicinity of nominal length 50 mm in order to analyze the influence of electromagnet length on electromagnetic force. Different armature lengths are shown in Figure 6(a).The effects of different armature lengths on electromagnetic force are shown in Figure 6(b).

Figure 6(b) shows that, with the increase of the armature length, the electromagnetic force increases gradually, but there is a peak value. The force decreases when the armature length is greater than the nominal length. Therefore, the optimum armature length in range of 30 mm-60mm is about 55 mm.

③ The influence of the rear angle of the iron core on electromagnetic force.

The structure of the electromagnet must be designed as a cone shaped shoe pole structure around the cone [12] in order to realize the proportional relation between the coil current and the electromagnetic force. Therefore, it is necessary to determine the size and geometry of the cup through the optimization design, in which the rear angle of iron core has a greater impact. The rear angles of different iron core are shown in Figure 7(a) and the influence of the different rear angles of iron core on electromagnetic force is shown in Figure 7(b).

Figure 7(b) shows that the corresponding electromagnetic force increases gradually when the rear angle of the iron core begins to increase from 0 degrees. The force reaches the maximum value when the rear angle reaches -40 degrees. Crossing through this point, the force decreases as increase of the angle. Therefore, the optimum angle of the iron core in the range of -60 degrees -0 degrees is -40 degrees.

④ The influence of secondary air gap on electromagnetic force.

The air gap in the electromagnet has a great influence on performance. The air gap is divided into the main air gap and the secondary air gap, as shown in Figure 8(a). The influence of the secondary air gap on the electromagnetic force is shown in Figure 8(b).

Figure 8(b) shows that the secondary air gap has a remarkable influence on electromagnetic force. The force surface of the armature decreases as the secondary air gap increases, so the optimum secondary air gap value in the range of 0.1mm-0.3mm is 0.1mm.

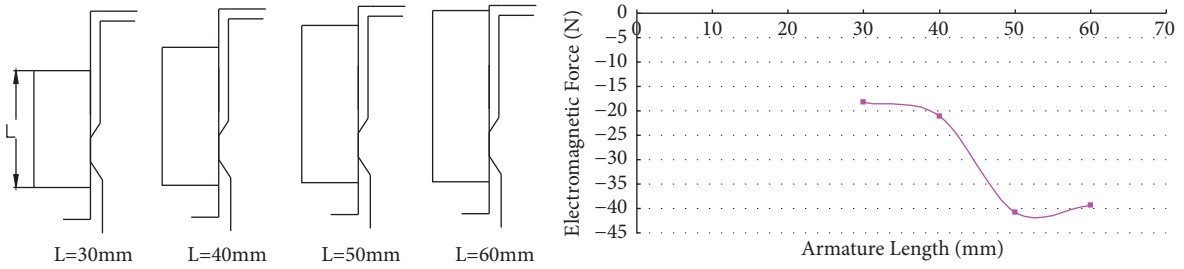

(a) Different armature length

(b) Change curve of electromagnetic force with armature length

Figure 6: Different armature lengths and their effect on electromagnet force.

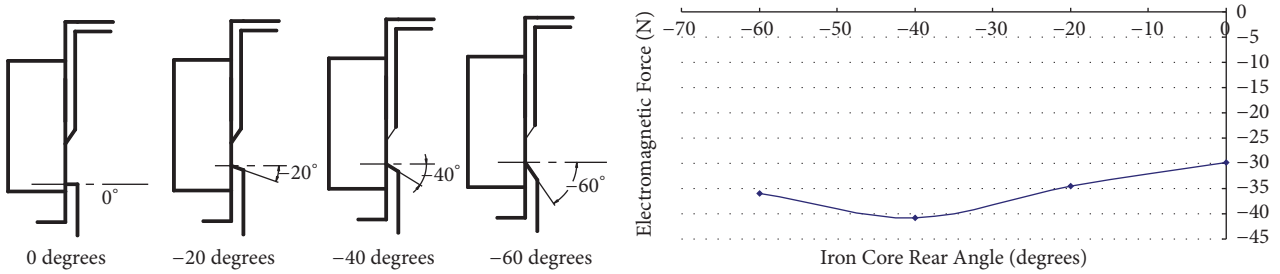

(a) Different rear angles of iron core

(b) Change curve of electromagnetic force with the rear angle of iron core

Figure 7: Different rear angles of iron core and the effect on electromagnet force.

3. Analysis of Coil Temperature Field of Electromagnetic Proportional Directional Control Valve

Research shows that one of the main failure forms of electromagnetic control valve is coil overheating, resulting in coil burnout [13]. The Ohm heat of coil is the main heat source. The thermal conductivity and specific heat capacity of material are the important factors affecting the temperature field of coil. The temperature field of electromagnetic proportional directional control valve varies in time and space and should be considered as a transient temperature field. Each of its periods can be regarded as steady state because the control valve works intermittently. The heat transfer process of electromagnetic proportional directional control valve mainly consists of heat conduction and convection heat transfer. It is a synthetical process of heat conduction and convection heat transfer.

The main internal heat of the electromagnet is heat conduction. The third order partial differential equation can be expressed as [14]

$$\frac{\partial}{\partial t}(\rho c T) - \operatorname{div}(\lambda \operatorname{grad} T) = \dddot{q} \tag{3}$$

where ρ is material density. c is material specific heat capacity. T is temperature. λ is material thermal conductivity. $\dddot{q}$ is heat generated by heat source in unit volume.

The first term of formula (3) is 0 if the steady-state temperature field is analyzed. Convection heat transfer in engineering applications can be calculated by the formula

$$q = \alpha_{conv} \bullet A \bullet \left(T_0 - T_f\right) \tag{4}$$

where q *is* heat flow. α_{conv} is convection heat transfer coefficient. A is heat transfer area. T_0 is heat source temperature.T_f is Fluid temperature.

ANSYS thermal module is used to solve above question.

(1) Preprocessing.

The steady-state temperature field of 2D is analyzed. The element type is PLANE55 and is axial symmetry [15]. The thermal conductivity of 0.7 and 0.032 is set, respectively, for coil and air [16]. The surface of the model is divided into quadrilateral free mesh, as shown in Figure 9.

(2) Loading two boundary conditions for the model.

① Define heat density of the internal heat source:

$$Q_V = \frac{I^2 R}{V_C} \tag{5}$$

where Q_V is the heat density. I *is* coil current. R is coil resistance. V_C is coil volume.

The coil heat generation rate is set as [17]

$$S = \frac{|J|^2}{\sigma} \tag{6}$$

where S is heat generation rate. σ is coil conductivity. J *is* coil current density.

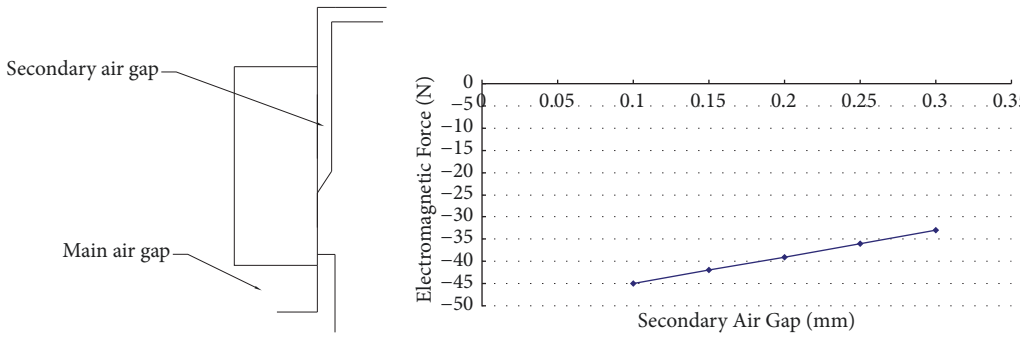

(a) Air gap (b) Change curve of electromagnetic force with secondary air gap

FIGURE 8: The secondary air gap and its effect on electromagnet force.

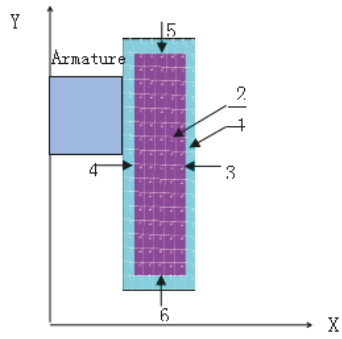

FIGURE 9: The coil meshing. (1) Air; (2) coli; (3) outer surface (faraway from armature); (4) inner surface (closed to armature); (5) upper surface; (6) lower surface.

In this paper, the parameter of the electromagnetic control valve is set the same as formula (1).

② Loading natural convection heat transfer coefficient.

The large space level natural convection heat transfer coefficient equation is used on upper surface 5 and the limited space horizontal natural convection heat transfer coefficient equation is used on lower surface 6. The vertical space natural convection heat transfer coefficient equation is used on outer surface 3 and the limited space vertical natural convection heat transfer coefficient is used on inner surface 4. The corresponding natural convection heat transfer coefficient of four surfaces is set in ANSYS as

$$\begin{aligned} \lambda_{upper} &= 12\mathrm{W/m^2 \bullet K}, \\ \lambda_{lower} &= 4\mathrm{W/m^2 \bullet K}, \\ \lambda_{outer} &= 8\mathrm{W/m^2 \bullet K}, \\ \lambda_{inner} &= 6\mathrm{W/m^2 \bullet K}. \end{aligned} \tag{7}$$

(3) The steady-state temperature analysis solver used to solve the problem.

(4) Postprocessing; viewing the results of the solution.

According to the formula (1) and formula (6), the factors that affect the coil heating include coil current, coil turn, and coil geometry. The heat generation rate of the coil can be reduced by reducing the coil current, the number of coil turns, and increasing the geometrical size of the coil, but the small coil current and coil turns will also affect the electromagnetic force. The opening requirements of control valve cannot be met if electromagnetic force is not enough, so the reliability is reduced. Therefore, coil temperature rise is studied from two aspects: the normal fluctuation of coil control current and the thermal conductivity of materials and the coefficient of convection heat transfer. The influence law is explored.

① The analysis results contrasted when the coil control current is 0.02A and 0.004A, respectively.

The coil is made of copper wire with an electrical conductivity of $5.9 * 10^7$S/m, as shown in Figure 10. The control current in the coil fluctuates between 0.004 and 0.02A when the control valve works. The maximum temperature at the center of the coil is 4.189 degrees centigrade and there is almost no temperature rise compared with the lowest temperature of the coil edge of 3.154 degrees when the control current in the coil is 0.004A, as shown in Figure 10(b). The maximum temperature of the coil center is 56.715 degrees centigrade when the control current in the coil is 0.02A. The temperature increases obviously, as shown in Figure 10(a). This can be explained by formula (5). The heat density of the inner heat source increases by square as the current increases and the heat energy increases, causing the coil temperature to rise. At the same time, the temperature at the center of the coil is higher than that at the edge of the coil because the heat source is in the center of the coil.

② The influence of coil thermal conductivity and convection heat transfer coefficient on coil temperature rise.

The thermal conductivity of the coil used in the previous analysis is a maximum value of 0.7, which is an ideal condition. In fact, the numerical value of the coil heat conduction coefficient is unknown and needs to be estimated and determined by the experimental results. In addition, compared with the natural air convection, the heat transfer coefficient of forced air convection increases, which can reach $20\,\mathrm{W/m^2 \bullet K}$. The thermal conductivity of the main insulation composed of different mica tapes can be measured by using the heat flux meter method [18, 19]. The

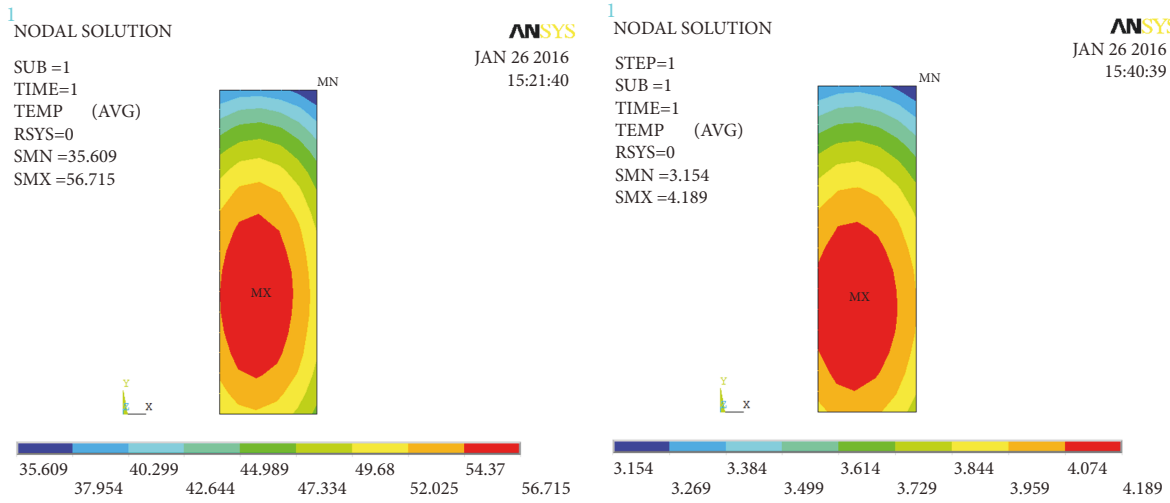

(a) I=0.02A (b) I=0.004A

Figure 10: Coil temperature field distribution.

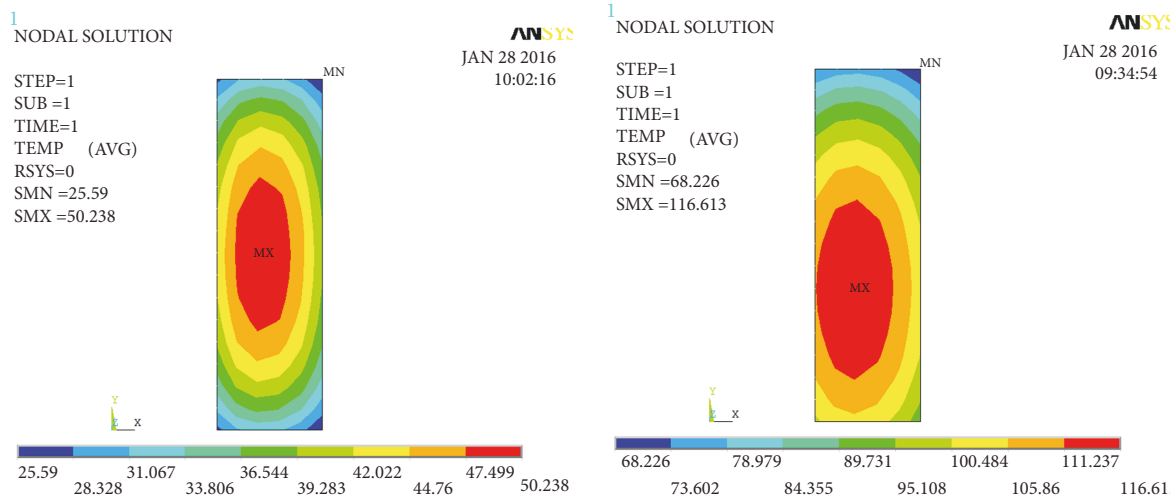

(a) High thermal conductivity and less rubber content mica tape (b) General more rubber content mica tape

Figure 11: The comparison of coil temperature field distribution.

results show that the thermal conductivity of insulation is proportionally increased with rubber content. The mica tape with high thermal conductivity and less rubber content can reach the highest thermal conductivity of 0.327 $W/m^2 \cdot K$ at 130 degrees centigrade while the thermal conductivity of general mica tap with more rubber content is 0.294 $W/m^2 \cdot K$ at 130 degrees centigrade. The temperature changes in the forced air convection of the coils with two different thermal conductivities and main insulations are compared and analyzed, as shown in Figure 11.

Figure 11 shows that the highest temperature in the center of the coil can be reduced from 116.613 degrees centigrade to 50.238 degrees centigrade using high thermal conductivity less rubber content mica tape as the main insulation material compared to general more rubber content mica tap under the forced air convection (such as cooling fan) heat transfer condition. The cooling effect is obvious and temperature distribution of the coil is basically symmetrical along upper and lower surface and inner and outer surface.

4. Conclusion

(1) Both the control current and the geometrical size of the electromagnet have influence on electromagnetic force. Firstly, coil control current, coil turns, the armature core length, rear angle, and secondary air gap should be designed reasonably to ensure enough electromagnetic force to drive the spool and improve the reliability of the control valve. Secondly, the electromagnetic proportional control valve is a multiphysics field coupled system, including electromagnetic field and flow field [20]. Therefore, the calculation of electromagnetic force should also consider the hydrostatic pressure,

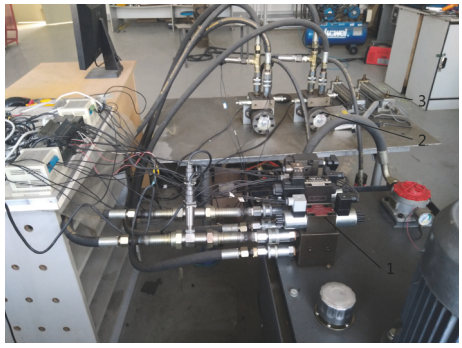

Figure 12: Hydraulic driven test bench of intelligent flexible sprayer chassis. (1) Electromagnetic proportional directional control valve; (2) hydraulic motor; (3) hydraulic cylinder.

the spring force, and damping force, so that the calculation results are more accurate.

(2) The coil temperature rise of the control valve is one of the key factors that affect its reliability. The coil temperature rise is mainly affected by the coil control current, the material thermal conductivity, and the heat transfer coefficient. The control valve used in this paper is not suitable for working full load current (0.02A) for a long time. Otherwise, the coil temperature rises and is easy to burn out. The forced air convection is better than the natural convection heat transfer and the coil has better heat dissipation effect. In addition, high thermal conductivity and less rubber content mica tape are used as main insulation materials and the temperature rise of the coil is obviously lower than that of the general more rubber content mica tape. The temperature can be reduced from 116.613 degrees centigrade to 50.238 degrees centigrade, which is beneficial to the improvement of the reliability of the electromagnetic proportional directional control valve.

(3) The optimized results are as follows: current intensity is 0.02A, the armature length is 55 mm, the rear angle of iron core is -40 degrees centigrade, and the secondary air gap is 0.1 mm besides adopting forced air convection and high thermal conductivity and less rubber content mica tape.

(4) Theoretical reference is provided for the reliability optimization design of the electromagnetic proportional directional control valve. The control valve optimized was used in the hydraulic driven test bench of intelligent flexible sprayer chassis. The speed of the hydraulic motor and hydraulic cylinder could be adjusted and controlled effectively by the control valve, shown in Figure 12. The electromagnetic force is enough to meet the flow and direction adjustment requirements and the temperature rise of the valve is below 50 degrees centigrade after working 1 hour, which is coincidental with simulation results.

Data Availability

The data used to support the findings of this study are included within the article.

Conflicts of Interest

The author declares that there are no conflicts of interest regarding the publication of this paper.

Acknowledgments

This research is supported by the Natural Science Research Project of Anhui Higher Education Institutions (Grant no. KJ2017A508), Stable Talent Project of Anhui Science and Technology University (Grant no. JXWD201701), and Anhui Excellent Young Talents Supporting Program Project (Grant no. gxyqZD2018068).

References

[1] W. Cai, X. Zheng, Z. Zhang, and X. Huang, "Failure mechanism analysis and transient characteristic simulation of hydraulic electromagnetic valve," *Chinese Journal of Scientific Instrument*, vol. 32, no. 12, pp. 2726–2733, 2011.

[2] F. Liang, D. Li, L. Hu, and J. Liu, "Simulation of the high-speed powerful solenoid valve in a high-pressure common-rail injection system for diesel engine," *Nongye Jixie Xuebao/Transactions of the Chinese Society of Agricultural Machinery*, vol. 36, no. 2, pp. 8–11, 2005.

[3] G. S. Lee, H. J. Sung, and H. C. Kim, "Multi-physics analysis of a linear control solenoid control valve," *Journal of Fluids Engineering*, vol. 135, no. 1, pp. 279–284, 2012.

[4] B. Sun, S. Gao, C. Ma, and J. Li, "System power loss optimization of electric vehicle driven by front and rear induction motors," *International Journal of Automotive Technology*, vol. 19, no. 1, pp. 121–134, 2018.

[5] X. Lu, Z. Liu, and Z. Lu, "Optimization design and experimental verification of track nonlinear energy sink for vibration control under seismic excitation," *Structural Control Health Monitoring*, vol. no.5, p. e2033, 2017.

[6] C. Zhou, R. Liang, and J. Zhang, "Optimization design method and experimental validation of a solar pvt cogeneration system based on building energy demand," *Energies*, vol. 10, no. 9, 2017.

[7] X. Luo, M. Wang, G. Dai, and X. Chen, "A Novel Technique to Compute the Revisit Time of Satellites and Its Application in Remote Sensing Satellite Optimization Design," *International Journal of Aerospace Engineering*, vol. 2017, Article ID 6469439, 9 pages, 2017.

[8] F. Bayat, A. F. Tehrani, and M. Danesh, "Finite element analysis of proportional solenoid characteristics in hydraulic valves," *International Journal of Automotive Technology*, vol. 13, no. 5, pp. 809–816, 2012.

[9] A. Lin, Z. Z. Liu, and L. Zhao, "Magnetic field analysis and electromagnetic force calculation for electromagnetic control valves based on finite element method," *Journal of Shandong University (Engineering Science)*, vol. 34, no. 6, pp. 27–31, 2004.

[10] J. S. Li, W. H. Hu, H. T. Lin, and H. P. Li, "Simulation analysis on static performance of EP solenoid control valves based on ANSYS," *China Railway Science*, vol. 26, no. 5, pp. 72–75, 2005.

[11] Y. X. Li, K. F. Zou, Y. Ou, Y. Guang, and D. S. Ou, "Finite element analysis of electromagnetic field and experimental study of high-speed solenoid for common rail injector," *Transactions of CSICE*, vol. 22, no. 6, pp. 549–554, 2004.

[12] F. Meng, G. Tao, and H. M. R. Zhang, "Optimization design and analysis of high speed wet proportional solenoid control valve," *Acta Armmmentarii*, vol. 35, no. 5, pp. 590–596, 2014.

[13] Z. W. Han, "Study on temperature field math model of driving coil of electromagnetism drive," *Micromotors*, vol. 44, no. 6, pp. 15–19, 2011.

[14] L. M. Huang, D. G. Chen, and J. S. Zhang, "Analysis of thermal field and transient thermal circuit of solenoid magnet by considering physical parameters as functions of temperatures," *Transactions of China Electro technical Society*, vol. 18, no. 5, pp. 27–31, 2003.

[15] B. Cai, Y. Liu, C. Ren, A. Abulimiti, X. Tian, and Y. Zhang, "Probabilistic thermal and electromagnetic analyses of subsea solenoid valves for subsea blowout preventers," *Strojniski Vestnik: Journal of Mechanical Engineering*, vol. 58, no. 11, pp. 665–672, 2012.

[16] Q. F. Liu, H. L. Bo, and L. Wang, "Analysis of temperature field of direct action solenoid control valve," *Nuclear Techniques*, vol. 36, no. 4, Article ID 040650, 2013.

[17] S. Y. Lin and Z. H. Xu, "Simulation and analysis on the three-dimensional temperature field of AC solenoid control valves," in *Proceedings of the CSEE*, vol. 32, pp. 156–164, 2012.

[18] H. Y. Zhu, "Measurement of thermal conductivity of the main insulation of stator windings in the turbine generator," *Motor Technology*, vol. 8, no. 2, pp. 48–50, 2014.

[19] Z. Y. Lin and X. Z. Chen, "Experimental determination and numerical simulation of the radial thermal conductivity of coils," *Mechanical and electrical engineering technology*, vol. 40, no. 8, pp. 79–82, 2011.

[20] Y. Liu, Z. Dai, X. Xu, and L. Tian, "Multi-domain modeling and simulation of proportional solenoid valve," *Journal of Central South University of Technology*, vol. 18, no. 5, pp. 1589–1594, 2011.